

# 1 Proper modelling of ligand binding requires an ensemble of bound 2 and unbound states

3 Nicholas M Pearce<sup>1</sup> and Frank von Delft<sup>1,2,3</sup>

4 1 Structural Genomics Consortium, University of Oxford, Roosevelt Drive, Oxford, OX3 7DQ, UK.

5 2 Diamond Light Source Ltd, Harwell Science and Innovation Campus, Didcot OX11 0QX, UK

6 3 Department of Biochemistry, University of Johannesburg, Auckland Park, 2006, South Africa

7 **Synopsis** We emphasise and demonstrate the importance of modelling the superpositions of ligand-  
8 bound and unbound states that commonly occur in crystallographic datasets. Generation of an ensemble  
9 that describes not only the dominant state in the crystal is important for the high-quality refinement of  
10 low-occupancy ligands, as well as to present a model that explains all of the observed density.

11 **Abstract** Small molecules bind to only a fraction of the proteins in the crystal lattice, but occupancy  
12 refinement of ligands is often avoided by convention; occupancies are set to unity, assuming that the  
13 error will be adequately modelled by the B-factors, and weak ligand density is generally ignored or  
14 attributed to disorder. Where occupancy refinement *is* performed, the superposed atomic state is rarely  
15 modelled. We show here that these modelling approaches lead to a degradation of the quality of the  
16 ligand model, and potentially affect the interpretation of the interactions between the bound ligand and  
17 the protein. Instead, superior accuracy is achieved by modelling the ligand as partially occupied and  
18 superposed on a ligand-free “ground-state” solvent model. Explicit modelling of the superposed  
19 unbound fraction of the crystal using a reference dataset allows constrained refinement of the occupancy  
20 of the ligand with minimal fear of over-fitting. Better representation of the crystal also leads to more  
21 meaningful refined atomic parameters such as the B-factor, allowing more insight into dynamics in the  
22 crystal. We present a simple approach and simple guidelines for generating the ensemble of bound and  
23 unbound states, assuming that datasets representing the unbound states (the ground state) are available.  
24 Judged by various electron density metrics, ensemble models are consistently better than corresponding  
25 single-state models. Furthermore, local modelling of the superposed ground state is found to be  
26 generally more important for the quality of the ligand model than convergence of the overall phases.

## 27 1. Introduction

28 Crystallographic diffraction experiments are used to reveal the atomic composition of protein crystals,  
29 but where the crystal is composed of objects in multiple states, the resulting diffraction pattern is a  
30 weighted average of these states. Ligands will often – and likely almost invariably – bind at sub-unitary  
31 occupancy; the subsequently derived electron density consists of an average over the bound state and  
32 the corresponding unbound state (which we term the *ground state*). However, it is standard practice not  
33 to model a superposition of multiple states, but instead to model only the ligand-bound conformation  
34 (and furthermore normally at unitary occupancy); this is commonly observed in the PDB<sup>1,2</sup> (Figure 1).

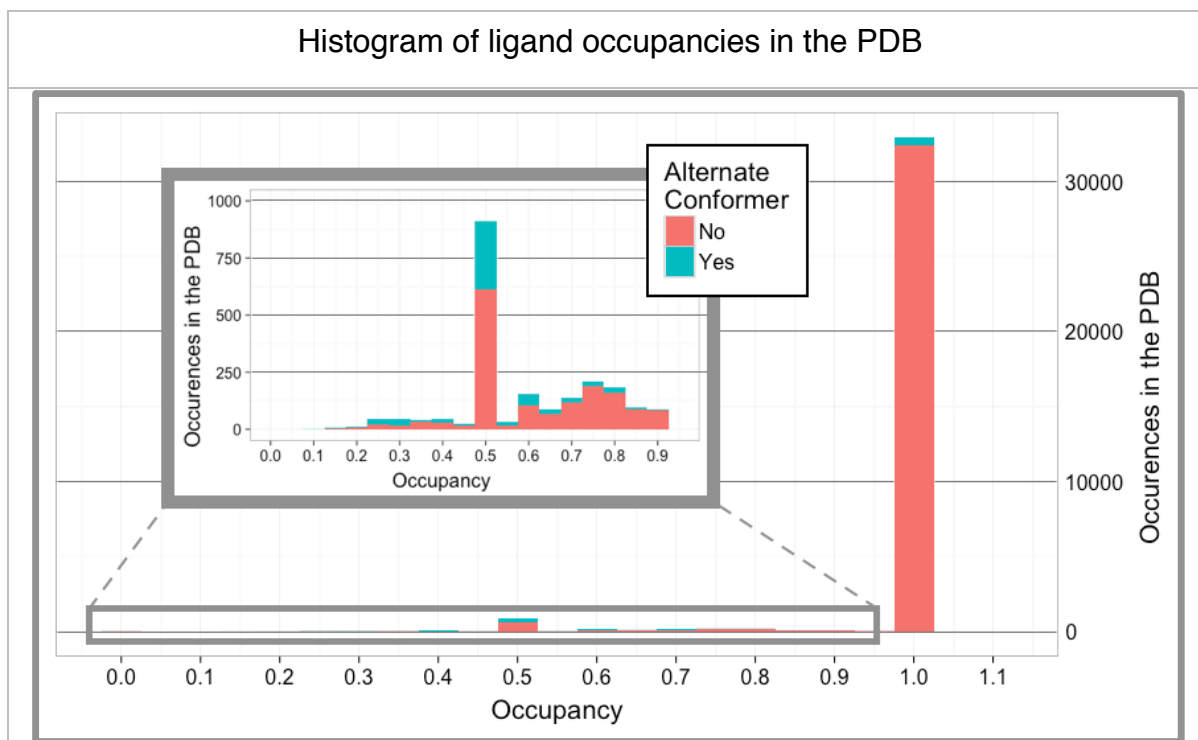


**Figure 1 Most ligands in the PDB are modelled at unitary occupancy, and many partial occupancy ligands are not modelled with an alternate state.** Histogram of all ligand occupancies in the PDB classified by the presence of an alternate conformer identifier (red: no conformer ID, blue: modelled with a conformer ID). Sub-unitary occupancy ligands are clarified in the inset graph. Only the first instance of each ligand type from each PDB structure was used; following this all ligands with fewer than 5 non-hydrogen atoms and more than 50 instances were removed to avoid bias towards common molecules. Where alternate conformations of ligands are present, the total occupancy is used. The large majority of ligands are modelled at unitary occupancy (32396, 92.1%). A smaller number have non-unitary occupancies but no alternate conformer identifier (1640, 4.7%). The remainder are modelled using alternate conformers (1122, 3.2%), of which 548 are ligands with alternate conformers that sum to unitary occupancy. Worryingly, there are also ten instances with more than 100% occupancy. These modelling statistics are unlikely to represent the true situation in crystal structures, where ligands will rarely bind at near-full occupancy; ligands will always have a superposed solvent model where present at partial occupancy.

36 Occupancy refinement of ligands is likely avoided due to well-known interdependencies, instabilities  
37 and ambiguities that can occur in the simultaneous refinement of both B-factors and occupancies:  
38 improvements in crystallographic model fit can equally well be achieved by reducing occupancy or  
39 increasing B-factors<sup>3</sup>. When ligands are modelled at full occupancy, any resulting error is absorbed by  
40 inflating the refined B-factors. One is led to conclude that occupancy refinement is only deemed  
41 necessary when difference density appears over the ligand model, an impression corroborated by  
42 multiple conversations in online discussion fora such as *ccp4bb* and *ResearchGate*.

43 If occupancy refinement of the ligand-bound state is performed without a superposed solvent model,  
44 this implicitly implies that the rest of the crystal is either represented by vacuum – which is highly  
45 unlikely – or by bulk solvent, depending on the refinement program used. Close to the surface of the  
46 protein, it is unlikely that the solvent is truly represented by a bulk solvent model; this is especially true  
47 of binding sites, where solvent and buffer molecules will often bind in an ordered fashion at high  
48 occupancy, as in the examples presented in section 4. The absence of a superposed solvent model is a  
49 glaring modelling omission, and here we set out to show that inclusion of the superposed unbound state  
50 not only leads to a more complete model of crystal, but to a higher quality ligand model.

## 51 **2. More complete models through explicit inclusion of the ground-state**

52 We propose that ligands will – in the general case – *always* be better modelled with explicit  
53 representation of the superposed solvent state, determined from a ground-state crystal of the protein.  
54 Inclusion of the ground-state allows the occupancy of the superposed states to be constrained in  
55 refinement, reducing the ambiguity from simultaneous refinement of b-factors and occupancies.

56 This approach requires a credible model of the ground-state to be available. This is indeed the case in  
57 a large proportion of ligand-binding experiments, where ground-state (ligand-free) crystals are easily  
58 obtained, e.g. experiments where ligands are “soaked” into pre-formed crystals. Where ground-state  
59 crystals are difficult to generate, e.g. where the ligand stabilises a particular protein conformation and  
60 thus crystal form, the assumption of an ensemble is in any case unlikely to be relevant.

61 Once the ground-state structure of the protein has been determined, the corresponding atoms can be  
62 directly transferred to the model of any subsequent dataset of the same crystal form. Specifically, the  
63 ground-state model is combined with the changed-state (ligand-bound) conformation, and refined as an  
64 ensemble. Generating this ensemble is algorithmically simple for datasets that are reasonably  
65 isomorphous; where this is not the case, the unbound structure would require local alignment of  
66 corresponding atoms, although methods to do this robustly do not currently exist, to our knowledge.

67 In-between cycles of reciprocal-space refinement – if the crystal system is highly isomorphous – the  
68 ensemble model can be modelled or visually validated in programs such as Coot<sup>4</sup> by alternating between  
69 real-space refinement of the ground-state model into a ground-state map (left-hand column, Figure 2),

70 and checking the validity of the complete model in the ligand-bound dataset. In the case of a PanDDA-  
71 determined model<sup>5</sup>, additional maps are available for the modelling of the ligand-bound conformation  
72 (right-hand column, Figure 2). The PanDDA implementation further performs automatic merging of  
73 the changed-state model and the ground-state model, allowing ensembles to be utilised with little  
74 additional effort.

75 During modelling and refinement, the ground-state model should be considered a Bayesian prior, such  
76 that the underlying ground-state structure is assumed not to change from crystal to crystal. This applies  
77 even if the ground-state is not clearly discernible in the electron density; minor states will be “masked”  
78 by superposed major states, but they will still remain except where the ligand is truly unitary occupancy.  
79 In cases where the ground-state structure is crystallographically ill-defined in the ligand-bound-dataset  
80 (such as at low-resolution) it may be necessary to restrain the ground-state model to the reference dataset  
81 during refinement<sup>6-8</sup>.

82 This restraint addresses the main risk inherent in ensemble approaches, namely over-modelling the  
83 observed density by including additional, unwarranted atoms: including the ground-state model has a  
84 strong, first-principles rationale, and the information is derived from independent measurements. While  
85 interpreting the remaining density may not be easy in general, methods such as PanDDA<sup>5</sup> address this  
86 problem explicitly by deconvoluting the superposition.

## 87 **2.1. Systematic labelling of multiple crystal states to maximise interpretability**

88 Locally heterogeneous crystal states are modelled through the use of alternate conformers, which  
89 ascribe each atom to a particular state of the crystal. Only for completely independent ensembles of  
90 models are alternate model identifiers utilised<sup>9</sup>. When merging the ground-state of the crystal with the  
91 ligand-bound state, the same conformer ID – sometimes referred to as the *altloc* or *altid* – should be  
92 given to all atoms of the same state. Each state may then be extracted by selection of a particular  
93 conformer from the ensemble, enabling the use of the structure by non-crystallographers; the  
94 superposed ground-state is essentially an experimental artefact. The occupancies of the different states  
95 may further be grouped during refinement, and the occupancies of the states constrained to sum to unity.

96 The clearest interpretation of the model is achieved when conformers are used for the bound and  
97 unbound states that are not used elsewhere in the structure; this prevents potential association of  
98 similarly-labelled alternate conformers that are causally unrelated. In the case of a single conformer for  
99 each bound/unbound state (where alternate conformers elsewhere in the structure, unrelated to binding,  
100 are A and B only), all ground-state-only atoms may be set to conformer C, and all bound-state-only  
101 atoms may be set to conformer D. This assignment of logical conformer IDs is automatically performed  
102 during the merging of the ground-state and the ligand-bound state within the PanDDA implementation;  
103 this automation greatly simplifies the modelling process, where the ground-state model is used as the  
104 starting model for analysis.

105 However, the limitations of alternate conformers can quickly manifest themselves where multiple  
106 conformations are present in the bound/unbound states. Since alternate conformers do not support  
107 branching of conformations (where e.g. an alternate conformation of the backbone can have two  
108 sidechain conformers), it may be necessary to introduce redundant alternate conformations for single-  
109 conformer residues to create contiguous models (Figure S1).

## 110 **2.2. Local model completeness versus overall phase quality**

111 Conventional crystallographic dogma states that high quality (near-convergence) phases are needed for  
112 the “optimal” crystallographic model to be obtained. However, we show in this work that the current  
113 convention of omitting the superposed unbound state is more detrimental to the quality of the ligand  
114 model than the degradation of the overall model phases. To compare the effects of global phase  
115 degradation, a “degraded-phase” model is produced in each of the examples in section 4. We begin with  
116 the final “optimal” model – where the ligand is modelled in superposition with a ground-state model –  
117 and distort the structure of the protein in regions distant from the ligand binding site, thereby introducing  
118 global phase error. Induced mean model phase difference relative to the full ensemble model is in the  
119 range of 20-30° (as calculated by `cphasematch`<sup>10</sup>). Further details may be found in section S1.

## 120 **3. Qualitative and quantitative comparison of different modelling approaches**

121 To demonstrate the improvement of ligand models through inclusion of the superposed ground state,  
122 we present four examples in section 4, covering a range of ligand occupancies. All ligands were  
123 identified with PanDDA Z-maps and ligand-bound states were modelled using the PanDDA event maps.  
124 Three models of the crystal containing ligands are refined and compared: a ligand-state-only model; a  
125 high-quality ensemble model; and a degraded-phase ensemble model. A solvent-state-only model is  
126 also refined for completeness (central column, Figure 2).

127 The ligand-state-only model for refinement is obtained by removing the ground state from the ensemble  
128 and setting the ligand occupancy to 0.95. The solvent-state-only model is similarly generated by  
129 removing the ligand-bound state and setting the solvent occupancy to 1.0 (this simulates the normal  
130 modelling case, where the solvent occupancy would not typically be refined). Degraded-phase models  
131 are created from the ensemble models as described in section 2.2. All models are refined with  
132 `phenix.refine`<sup>11</sup> (version 1.9-1682) using the default parameters against crystallographic data from  
133 before a ligand was placed, to prevent phase bias. Ligand occupancy is refined for all models; for the  
134 ensemble models, the occupancies of superposed states are constrained to sum to unity.

### 135 **3.1. Utilisation of validation metrics for quantitative model comparison**

136 The refined ligand models are compared using a variety of density- and model-based validation metrics;  
137 these metrics and their optimal values are described in Table 1. Density metrics – all calculated by

138 EDSTATS<sup>12</sup> – include the conventional real-space correlation coefficient (RSCC), but also newer  
139 metrics such as RSZD and RSZO<sup>12</sup>. Tickle (2012) shows that these new metrics can be used to ask more  
140 detailed questions about the model: RSZD measures the accuracy of the model through the analysis of  
141 difference density, highlighting modelling errors, and RSZO measures the precision of the density for  
142 the model, highlighting weak features. RSZO is calculated by taking the average of the density over the  
143 model and dividing by the noise in the map; since the amount of density for a residue is directly related  
144 to the occupancy of the residue, we divide RSZO by the occupancy of the residue to give a normalised  
145 value (RSZO/OCC) that can be used to compare models at different occupancies in the same dataset.  
146 We also calculate the B-factor ratio of the ligand to the surrounding protein residues (within 4Å) to  
147 measure the consistency of the ligand model with its local environment; as well as the RMSD of the  
148 refined ligand and the fitted ligand, to measure the (in)stability of the model coordinates in refinement.  
149 These measures are displayed visually as radar plots, where the “better” the metric value, the closer it  
150 is to the centre of the plot. The axes of the radar plot are scaled such that the “best” value is plotted at  
151 the centre of the plot and the “worst” value is plotted at the extreme of the axis.  
152

**Table 1 Electron density and model metrics used for the validation of crystallographic models.** The combination of five metrics highlights a variety of features of models, and together allow for a comprehensive description of the atomic model of a residue. RSCC ensures good overall similarity of the model to the density. RSZD measures the difference density over the model, highlighting errors or the presence of currently un-modelled or over-modelled atoms. RSZO indicates density strength, and the normalisation by occupancy can indicate errors in the occupancy of a model or a misplaced or absent model. The B-factor ratio highlights errors in the B-factors of a residue, as these should be consistent with its surroundings: physically, there cannot be step changes in mobility of atoms in a crystal. The RMSD measures the movement of residues in refinement; a numerically unstable residue may be indicative of error in the model. All density metrics are calculated using EDSTATS<sup>12</sup>.

Metric	Description	Preferred values
RSCC	Correlation between model and observed electron density	> 0.7
RSZD	Statistical measure of difference density in region of model	< 3
RSZO/OCC	Strength of density over model, normalised for occupancy	> 2
B-factor Ratio	B-factor ratio of residue atoms and sidechain atoms within 4Å	~ 1
RMSD	Root-mean-squared-deviation of the atomic coordinates	< 1

153

### 154 **3.1.1. Effects of phase quality on model validation metrics**

155 The RSZD metric is less informative when analysing models with poor phases, because it is dependent  
156 on the quality of the model phases. RSZD and RSZO are derived with the assumption of near-  
157 convergence phases, and use an estimation of the noise in the maps to calculate quality criteria for  
158 residues. Lower RSZD would normally indicate a better model, but this is not the case here: when the  
159 quality of the phases is reduced, the noise in the maps also increases, and therefore decreases both  
160 RSZD and RSZO, regardless of whether the model has changed.

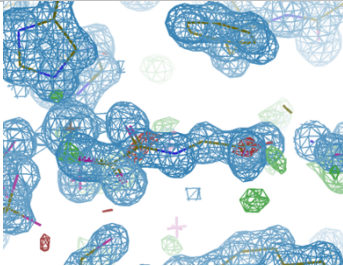
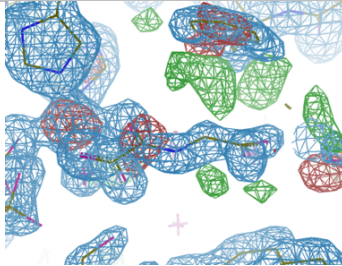
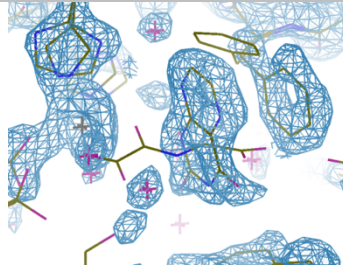
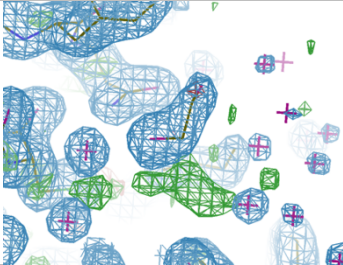
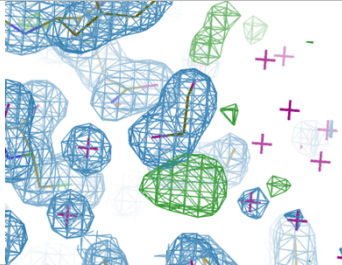
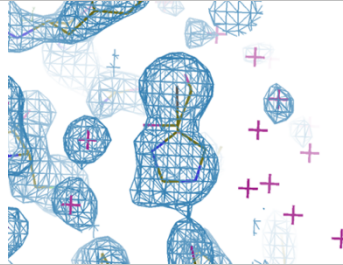
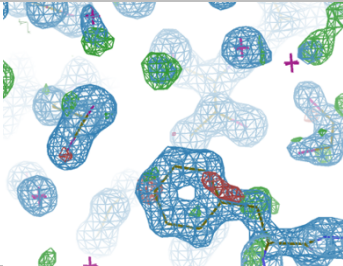
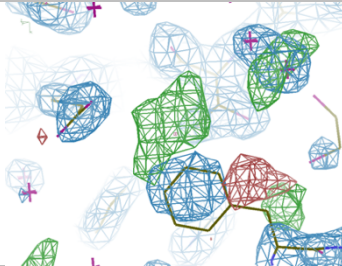
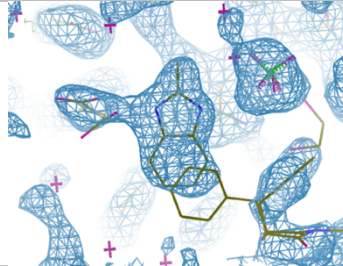
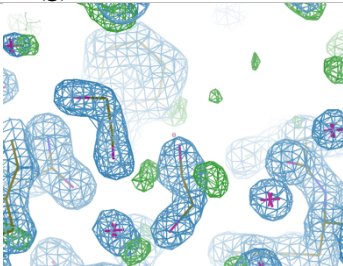
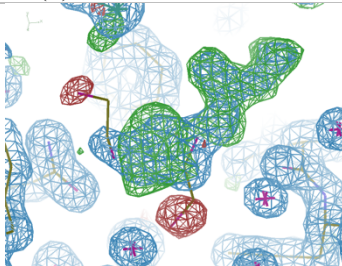
## 161 **4. Results**

162 We now present several cases where the inclusion of a complementary solvent model leads to a better  
163 description of the crystal, and thereby a higher-quality ligand model. The models here were all identified  
164 and modelled using the PanDDA method<sup>5</sup>. The model of the ligand was in each case derived from  
165 PanDDA “event” maps, and we investigate here only the effect that the inclusion/absence of the  
166 superposed solvent model has on the interpretation of the data. Models are generated and refined as  
167 described in previous sections. Validation metrics are calculated for only the ligand residue in each of  
168 the models. Crystallographic model parameters, including ligand validation scores, may be found in  
169 section S1. Details for obtaining the crystallographic data can be found in the PanDDA publication<sup>5</sup>.

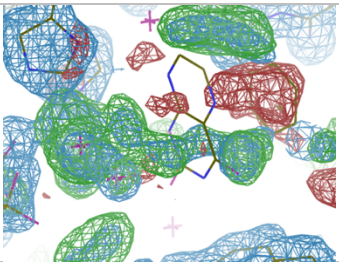
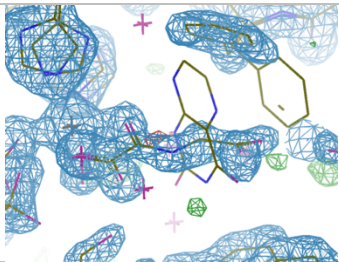
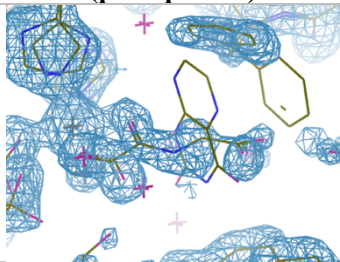
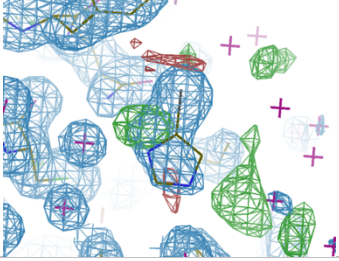
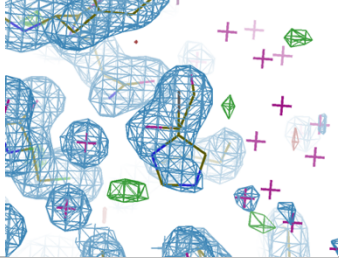
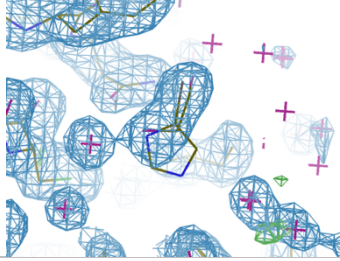
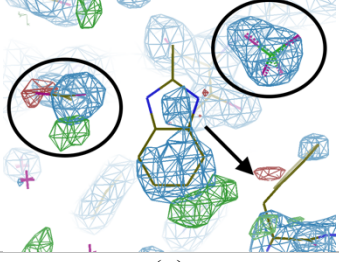
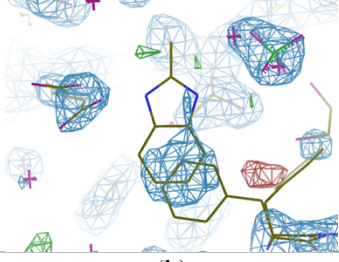
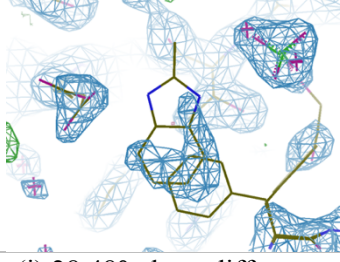
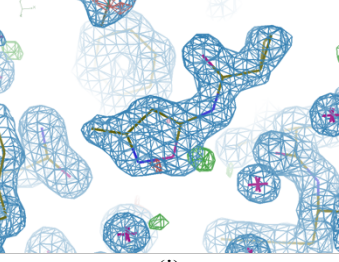
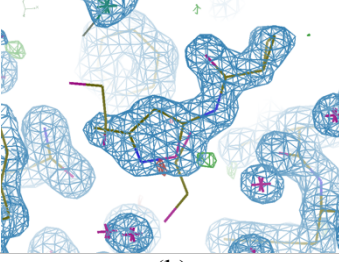
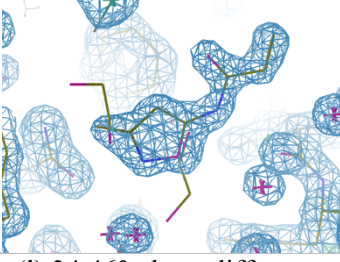
### 170 **4.1. Binding of the ligand across a bound substrate mimetic**

171 To demonstrate the process of modelling both states, we first present an example where a strongly  
172 bound substrate mimetic is superposed with a weakly-bound soaked ligand, and an ensemble is clearly  
173 necessary. N-oxalylglycine (NOG) is tightly bound at high occupancy (~90%) in the ground-state  
174 crystal form of human Lysine-specific demethylase 4D (KDM4D), as shown in the reference dataset  
175 (Figure 2a). A soaked ligand binds across this substrate mimetic in a small fraction of the crystal, as  
176 shown in the PanDDA event map (Figure 2c). Modelling of the two states can thus be performed  
177 separately, and merged for refinement; when refined as an ensemble, the superposition of the two states  
178 leads to a good model, with negligible amounts of difference density remaining (Figure 3b).

179 Although not interpretable, residual difference density can still be seen for the bound ligand when the  
180 ground-state model is refined alone (Figure 2b). As expected, refinement of the ligand without the  
181 superposed NOG results in a poor quality model (Figure 3a), because a large fraction of the crystal is  
182 locally unrepresented; refinement of the ensemble results in a better model for the ligand (Figure 3b),  
183 scoring well across all 5 metrics. On the radar validation plot (Figure 4a) this is shown as the ensemble-  
184 model line (green) being entirely contained within the ligand-only line (red) – the closer the line is to  
185 the centre of the plot, the better the model. Optimal modelling of the ligand requires the superposed  
186 ground-state conformation to be present in refinement.

Protein	Ground-state only (reference dataset)	Ground-state only (ligand-bound dataset)	Ligand-bound state (PanDDA event map)
KDM4D	 (a) dataset x618; 1.14Å	 (b) dataset x401; 1.48Å	 (c) dataset x401
BAZ2B	 (d) dataset x645; 1.49Å	 (e) dataset x538; 1.77Å	 (f) dataset x538
KDM4D	 (g) dataset x618; 1.14Å	 (h) dataset x568; 1.97Å	 (i) dataset x568
BRD1	 (j) dataset x108; 1.38Å	 (k) dataset x049; 1.46Å	

**Figure 2 Determining the different crystal states requires different datasets.** First two columns:  $2mF_o-DF_c$  maps contoured at  $1.5\sigma$  (blue) and  $mF_o-DF_c$  maps contoured at  $\pm 3\sigma$  (green/red). Last column: PanDDA event maps (blue) contoured at (c,f)  $2\sigma$  or (i)  $1\sigma$ . Resolutions are as indicated. First column: A reference dataset provides the ground-state model of the crystal. Centre column: The ground-state refined into a ligand-bound dataset leaves (generally uninterpretable) residual density for a superposed state. Last column: The PanDDA event map provides clear density for the ligand-bound model of the crystal (the superposed ground-state model is shown for reference). (a-c) Example from section 4.1. (d-f) Example from section 4.2. (g-i) Example from section 4.3. (j-k) Example from section 4.4; the event map is not shown since it is not required.

Protein	Ligand-bound state only	Ensemble model	Ensemble model (poor phases)
<b>KDM4D</b> dataset x401			
	(a)	(b)	(c) 24.17° phase difference
<b>BAZ2B</b> dataset x538			
	(d)	(e)	(f) 31.06° phase difference
<b>KDM4D</b> dataset x568			
	(g)	(h)	(i) 28.48° phase difference
<b>BRD1</b> dataset x049			
	(j)	(k)	(l) 34.46° phase difference

**Figure 3 Ensemble models consistently leave less residual difference density than ligand-only models.** All images:  $2mF_o-DF_c$  maps contoured at  $1.5\sigma$  (blue) and  $mF_o-DF_c$  maps contoured at  $\pm 3\sigma$  (green/red). First column: Refinement with the ligand model only. Centre column: Refinement of the crystal as an ensemble of states. Last column: Refinement of the crystal as an ensemble of states with a degraded protein model (phase difference as indicated, relative to the ensemble model). (a,d,g) Modelling the ligand but removing the ground-state leads to difference density for the absent state, and in (d) the ligand moves into density for the ground-state. (j) Removing the ground-state for a high occupancy ligand (refined value 0.89) does not lead to discernible difference density. (b,e,h,k) Refinement of ensemble models explain all of the observed density, and ligands do not move from the fitted pose (confirmed by the validation plots in Figure 4). (c,f,i,l) Refining with degraded phases leads to only minor visual differences, except in (f) where the ligand moves relative to the fitted pose.

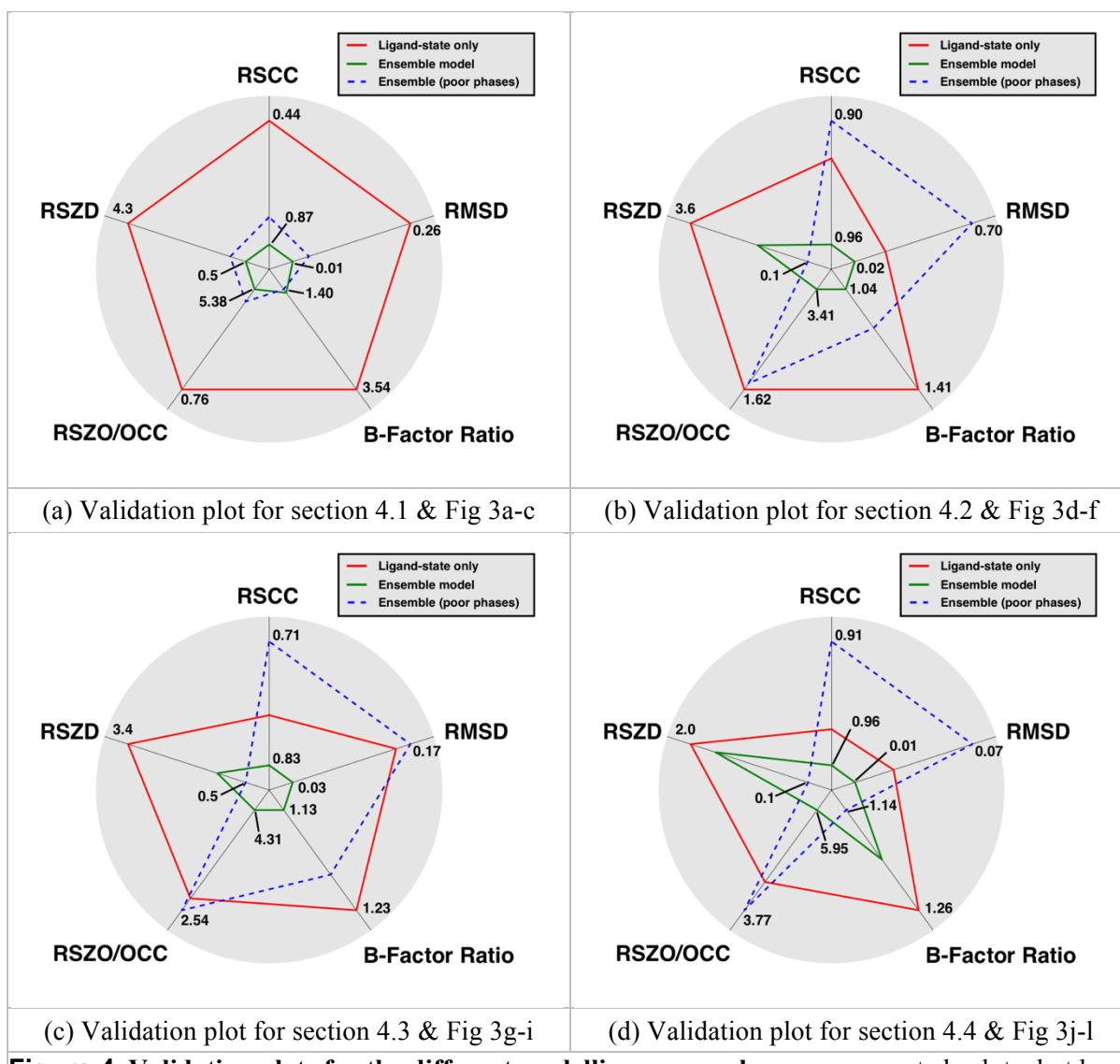


**Figure 4 Validation plots for the different modelling approaches:** axes are not absolute, but have been scaled relative to minima and maxima of the plotted values, and only the minimum and maximum values are marked on the axes; for all model scores refer to section S1. (a) Plots for Figure 3a-c. The plot confirms the visual inspection of the electron density; the ligand scores are improved across all metrics when refined as an ensemble, relative to the ligand modelled alone. The absence of the superposed substrate model has a greater effect on the ligand model than the degradation of the protein model phases. (b) Plots for Figure 3d-f. The ensemble model provides the best model for the ligand. The RSZD is decreased in the degraded-phase model for reasons explained in the main text, and is not related to an improved model. (c) Plots for Figure 3g-i. Once more, the model statistics are improved with the addition of a superposed solvent model, with the caveat that the lower RSZD for degraded phases is not indicative of an improved model. (d) Plots for Figure 3j-l. The inclusion of the solvent model still increases the quality of the model compared to when it is omitted, albeit marginally. The degraded phase model has lower B-factor ratios than either of the other two models due to a decrease in the B-factors of the ligand and a corresponding drop in occupancy.

190 The degraded protein model (Figure 3c) has a  $31^\circ$  average phase difference to the high-quality ensemble  
191 model, increasing the R-free from 17% to 29%. However, the model of the ligand is not significantly  
192 degraded, and still scores well on all five model validation metrics, although worse than the ensemble  
193 model with high-quality phases. In this case, the correctness of the local model is more important than  
194 the convergence of the global phases.

## 195 **4.2. Binding of a ligand in place of a solvent molecule**

196 In a soaked crystal of human Bromodomain Adjacent to Zinc finger domain 2B (BAZ2B), an ethylene  
197 glycol is bound in a semi-ordered fashion, with a superposed ligand, to the asparagine in the binding  
198 site. The solvent model derived from a reference dataset is not optimal, and some difference density  
199 remains even when a ligand is not present (Figure 2d). Refinement with the ground-state model in the  
200 ligand-bound dataset does not lead to significant additional difference density, as the refined solvent  
201 model masks the presence of the ligand's bromine (Figure 2e).

202 The PanDDA map, however, shows clear evidence for the ligand (Figure 2f); the positioning of the  
203 bromine can also be confirmed by an anomalous difference map (not shown). Refinement with only the  
204 bound state causes the ligand atoms to be pulled into the density for the ethylene glycol, and difference  
205 density remains (Figure 3d). Refinement of the ensemble leads to a good model (Figure 3e), with all  
206 density well-explained, and no movement of the ligand from the fitted pose.

207 Refinement of the degraded-phase model (Figure 3f) also causes the ligand to move relative to the fitted  
208 position. In this case, the absence of the superposed model and the quality of the model phases are both  
209 important for the quality of the final ligand model, reflected by the validation metrics (Figure 4b).

210 It is noteworthy that the RSCC of the ligand in all models is greater than 0.9, showing that whilst a large  
211 RSCC is necessary for a good model, it is not sufficient to determine the quality of the model: it does  
212 not account for the presence of difference density. As explained in Section 3.1.1, the RSZD of 0.1 for  
213 the degraded-phase ligand model, which would normally indicate a very good model, is affected by  
214 noise in the maps from the degraded phases; the RSZD is very sensitive to the overall correctness of  
215 the model. Multiple validation metrics, as well as a near-complete model, are needed to validate weak  
216 features.

## 217 **4.3. A binding ligand overlaps with alternate conformations of a sidechain**

218 Another ligand in a KDM4D dataset binds along with a sulphate to a putative allosteric site. Refinement  
219 with the ground-state conformation leaves residual unmodelled difference density (Figure 2g,h). The  
220 pose and identity of the ligand is clearly revealed in the PanDDA event map (Figure 2i), revealing the  
221 re-ordering of two sidechains and that the ligand is superposed on the ground-state conformation of the  
222 phenylalanine.

223 Upon inspection of the refined ensemble model (Figure 3h), it was suggested to the authors by another  
224 experienced crystallographer that the ground-state conformation should be deleted and the ligand-bound  
225 state refined as the sole conformation. This recommendation supports our observation that the pervading  
226 convention – to generate only a single conformation of the crystal wherever possible – dominates even  
227 in the face of clear evidence that multiple states are present. The density in the area of overlap between  
228 the ligand and the phenylalanine is significantly stronger than over the rest of either residue, and  
229 difference density is present when either state is refined separately (Figure 2h, Figure 3g). The residual  
230 density from the ligand-state-only model (Figure 3g) might further tempt a crystallographer to move  
231 the model down and right by  $\sim 1\text{\AA}$  (as indicated by the arrow in Figure 3g), although this causes clashes  
232 with the  $C_{\beta}$  of the phenylalanine and adversely affect the interactions that the ligand makes with the  
233 aspartate and the sulphate (marked with ovals in Figure 3g). All evidence points towards the presence  
234 of multiple states in the data, and therefore these multiple states should be present in the model.

235 The phase degradation in Figure 3i (mean phase difference to ensemble model  $28.48^{\circ}$ ) degrades the  
236 ligand model RSZO and the B-factor ratio to a similar level as the omission of the ground state model,  
237 and significantly degrades the RSCC (Figure 4c). Again, we observe a decrease in RSZD with the  
238 decrease in phase quality. The ensemble model provides the best interpretation of the experimental data.

#### 239 **4.4. Traces of the ground state remain, even for a high occupancy ligand**

240 One ligand screened against the bromodomain of BRD1 binds strongly in the principal binding site  
241 (Figure 2j,k), with a refined occupancy of 84-89% (multi-state and ligand-only refined occupancies  
242 respectively). In the reverse case of section 4.1, the ligand occupancy is much higher than the ground-  
243 state occupancy, and this ligand would conventionally be modelled at unitary occupancy.

244 Once more, inclusion of the ground-state solvent improves the model quality, although in this case only  
245 marginally (Figure 3j,k & Figure 4d). Even with this strong binder, visual traces of the ground-state  
246 model remain: contouring the  $2mF_o-DF_c$  map to zero rmsd shows some evidence for ground-state  
247 solvent (Figure 5).

248 Phase degradation degrades the RSCC, RMSD and the RSZO more than the absence of the solvent  
249 model, with a decrease in RSZD as previously. Here the B-factor ratio is seen to be lower for the phase-  
250 degraded model than for the other models, due to a decrease in the B-factors of the ligand by two, and  
251 a corresponding decrease in the occupancy to 0.77; this behaviour demonstrates the ambiguity that can  
252 be observed in simultaneous refinement of B-factors and occupancies.

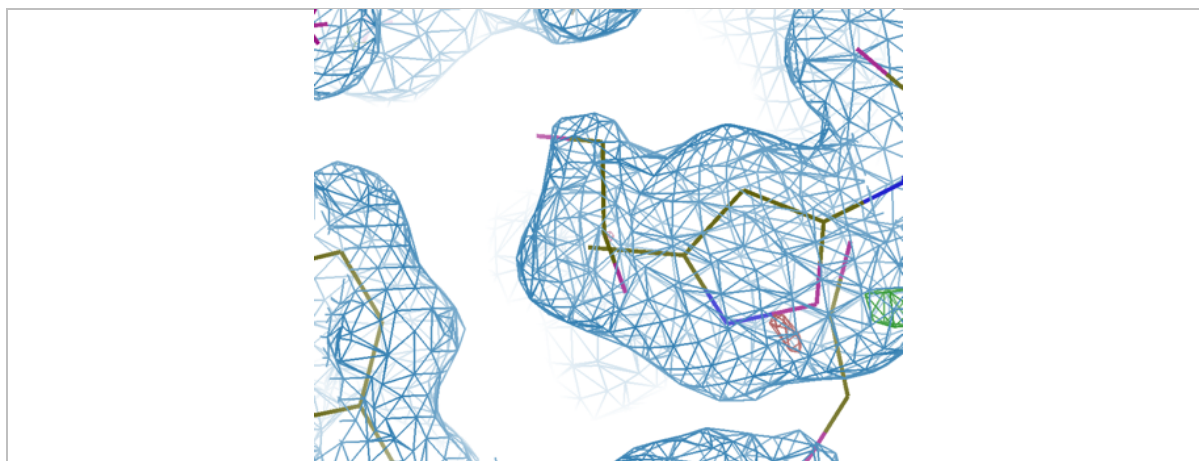


**Figure 5** Weak density for the ground-state model is still visible in refined maps. No evidence is seen that would support the removal of the superposed solvent model.  $2mF_o-DF_c$  map (blue) contoured at  $0.0\sigma$ ,  $mF_o-DF_c$  map (green/red) contoured at  $\pm 3\sigma$ .

## 253 5. Discussion

254 The examples presented here show that there is consistent evidence that ground-state molecules are  
255 superposed in the experimental data on top of binding ligands across a range of non-unitary  
256 occupancies. We have also shown that the inclusion of a superposed ground-state model, obtained from  
257 a reference dataset, improves the quality of obtained ligand models in all cases. In the case of some  
258 weak ligands, the ground state model is crucial for the refinement of the protein/ligand complex (section  
259 4.1); in other cases it acts simply to remove “extraneous” difference density that could be interpreted  
260 by an over-zealous modeller as being caused by a ligand in multiple conformations (section 4.2). The  
261 modelling approach can affect the interpretation of inter-molecular interactions (section 4.3), and in the  
262 case of high occupancy, a superposed ground state can still marginally improve the ligand model,  
263 alongside providing a complete model of the crystal (section 4.4).

264 With the current increase in popularity of experiments such as fragment screening by crystallography  
265 amongst academic groups, the PDB is set to see a sharp increase in structures that contain binders with  
266 considerably less than unitary occupancy (e.g. [13]). We have shown that the models of such partial-  
267 occupancy ligands benefit from the inclusion of a superposed ground-state; from these results, we  
268 propose that a new standard modelling convention is adopted, where bound ligands are modelled as a  
269 superposition of states *wherever possible*. Experimentally this is no extra burden, as an unbound  
270 reference dataset is normally already available when soaking experiments are performed.  
271 Computationally, however, this will require the implementation of tools for the trivial generation of  
272 ensembles from multiple single-state models; the PanDDA implementation goes some way towards  
273 achieving this new paradigm.

274 Performed correctly, the addition of a solvent model allows no further degrees of freedom for the  
275 crystallographer, as the ground-state model is solely determined in an orthogonal reference dataset.

276 Utilisation of prior knowledge in the modelling process will lead to higher quality crystallographic  
277 phases, and should ultimately contribute to closing the R-factor gap<sup>14</sup>.

278 We further propose that the ground-state should only be removed from the ensemble model if the  
279 occupancy of the refined ground-state conformer is  $\lesssim 10\%$  – only in this case is the benefit of the  
280 ground-state model in refinement likely negligible. *We should assume that the ground-state is present*  
281 *in the ligand-bound crystal until it is proven absent*; this is contrary to the current convention, which  
282 appears to assume the opposite.

283 Correct parameterisation of the ensemble model can lead to complicated models and refinement  
284 constraints that are currently not supported by some refinement programs (REFMAC<sup>15</sup>,  
285 phenix.refine<sup>11</sup>): in some cases not shown here, we have found that refinement of multiple conformer  
286 models permitted occupancies for amino acids that summed to greater than unity. Further work will be  
287 required to generate occupancy and structural restraints that allow complex ensemble refinement in the  
288 general modelling case, without permitting unphysical atomic models. Procedural generation of  
289 ensembles and the corresponding parameterisation files will be critical to the uptake of this approach.

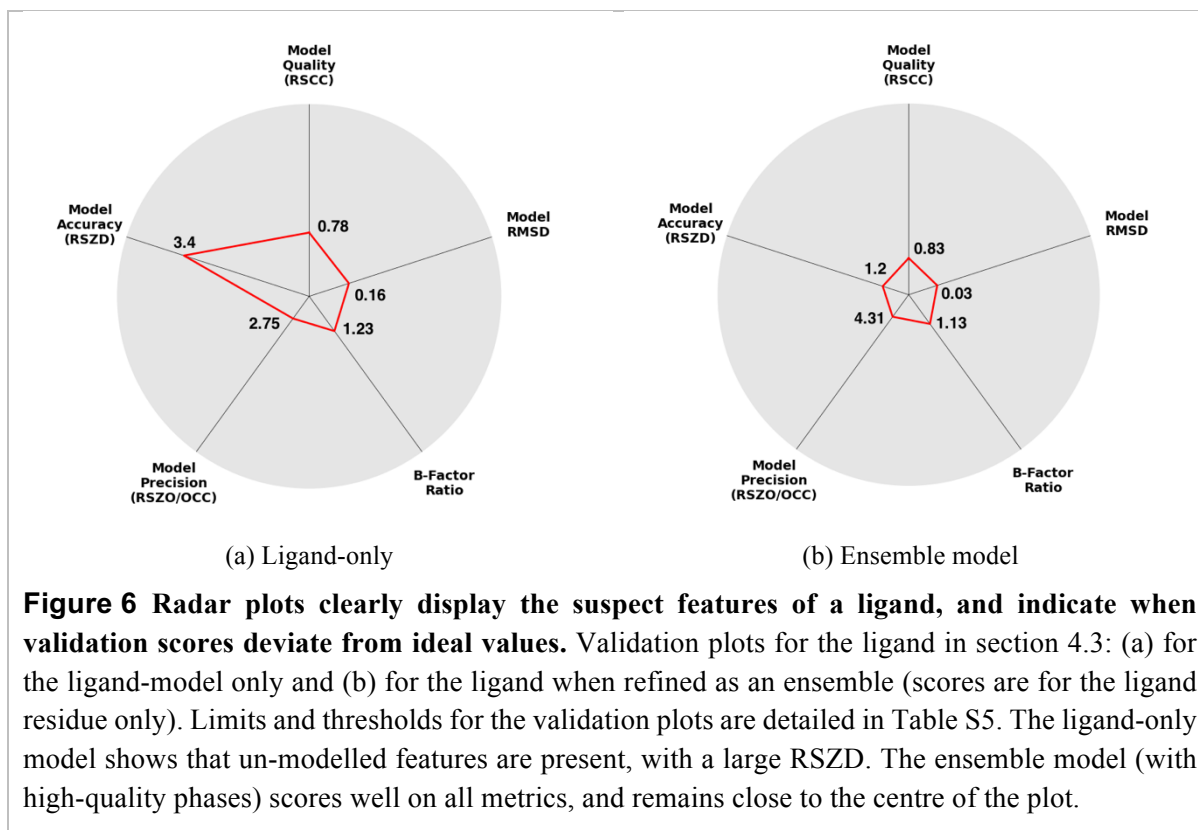
290 The examples shown here also highlight that RSCC alone is not enough to assess the quality of a ligand  
291 model: RSZD and RSZO should be used to ensure things have been modelled correctly, but require  
292 phases to be near convergence; a small B-factor ratio indicates consistency with the ligand's  
293 environment; and a small RMSD measures stability in refinement. The combination of a normalised  
294 RSZO and B-factor ratio further allow the stability of B-factor and occupancy refinement to be  
295 analysed; imbalances between these two metrics are a good indication of imbalance in the occupancy  
296 and the B-factors. The radar plots present the validation metrics clearly, and may be a useful tool for  
297 the validation of ligands in general. In this manuscript, we have used the validation plots to compare  
298 multiple models, and to this end, the plot axes were re-scaled to cover the range of the data. However,  
299 we propose that a more general use of the radar plot is to show when the ligand scores depart from ideal  
300 values (the proposed ranges for the metrics are shown in section S2); examples are shown in Figure 6  
301 for the ligand in section 4.3.

302 Lastly, we have investigated the impact of phase degradation on ligand model quality, compared to the  
303 effect of local modelling. We conclude that the modelling of local ground-state atoms is generally far  
304 more important than convergence of the global model, especially as global errors in typical modelling  
305 situations are likely to be much less than the  $\sim 30^\circ$  phase error introduced here. “Tweaking” of sidechain  
306 conformations and water molecules in distant regions in the model to improve phases is likely not of  
307 importance if the binding of a ligand is the feature of interest. However, the modelling of the  
308 environment around and “under” the ligand is conversely of great importance.

309 Recent reports have emphasised the importance of achieving maximally correct phases for more reliable  
310 interpretation of weak difference density<sup>13</sup>. Instead, this work indicates that the main rationale for doing

311 so is to ensure the validation metrics are reliable – as ligand identification can be performed without  
312 optimal phases<sup>5</sup> – and that the refinement of occupancy and B-factors is stable (as demonstrated in  
313 section 4.4).

314



315

316 **Acknowledgements** NMP would like to recognize funding from EPSRC grant EP/G037280/1, UCB  
317 Pharma and Diamond Light Source. Crystallographic data were collected by Anthony Bradley, Patrick  
318 Collins, Romain Talon and Tobias Krojer at Diamond Light Source, Beamline i04-1. The SGC is a  
319 registered charity (No. 1097737) that receives funds from AbbVie, Bayer, Boehringer Ingelheim, the  
320 Canada Foundation for Innovation, the Canadian Institutes for Health Research, Genome Canada,  
321 GlaxoSmithKline, Janssen, Lilly Canada, the Novartis Research Foundation, the Ontario Ministry of  
322 Economic Development and Innovation, Pfizer, Takeda and the Wellcome Trust (092809/Z/10/Z).

323

## 324 References

- 325 1. Berman, H. M. *et al.* The Protein Data Bank. *Nucleic Acids Res.* **28**, 235–42 (2000).
- 326 2. Berman, H., Henrick, K. & Nakamura, H. Announcing the worldwide Protein Data Bank. *Nat.*  
327 *Struct. Biol.* **10**, 980 (2003).

- 
- 328 3. Bhat, T. N. Correlation between occupancy and temperature factors of solvent molecules in  
329 crystal structures of proteins. *Acta Crystallogr. Sect. A* **45**, 145–146 (1989).
- 330 4. Emsley, P., Lohkamp, B., Scott, W. G. & Cowtan, K. Features and development of Coot. *Acta*  
331 *Crystallogr. Sect. D Biol. Crystallogr.* **66**, 486–501 (2010).
- 332 5. Pearce, N. *et al.* A Multi-Crystal Method for Extracting Obscured Signal from  
333 Crystallographic Electron Density. *bioRxiv* (2016).
- 334 6. Smart, O. S. *et al.* Exploiting structure similarity in refinement: Automated NCS and target-  
335 structure restraints in BUSTER. *Acta Crystallogr. Sect. D Biol. Crystallogr.* **68**, 368–380  
336 (2012).
- 337 7. Nicholls, R. A., Long, F. & Murshudov, G. N. Low-resolution refinement tools in REFMAC5.  
338 *Acta Crystallogr. Sect. D Biol. Crystallogr.* **68**, 404–417 (2012).
- 339 8. Headd, J. J. *et al.* Use of knowledge-based restraints in phenix.refine to improve  
340 macromolecular refinement at low resolution. *Acta Crystallogr. Sect. D Biol. Crystallogr.* **68**,  
341 381–390 (2012).
- 342 9. Burnley, B. T., Afonine, P. V., Adams, P. D. & Gros, P. Modelling dynamics in protein crystal  
343 structures by ensemble refinement. *Elife* **1**, e00311 (2012).
- 344 10. Winn, M. D. *et al.* Overview of the CCP4 suite and current developments. *Acta Crystallogr.*  
345 *Sect. D Biol. Crystallogr.* **67**, 235–242 (2011).
- 346 11. Afonine, P. V. *et al.* Towards automated crystallographic structure refinement with  
347 phenix.refine. *Acta Crystallogr. Sect. D Biol. Crystallogr.* **68**, 352–367 (2012).
- 348 12. Tickle, I. J. Statistical quality indicators for electron-density maps. *Acta Crystallogr. Sect. D*  
349 *Biol. Crystallogr.* **68**, 454–467 (2012).
- 350 13. Schiebel, J. *et al.* High-Throughput Crystallography: Reliable and Efficient Identification of  
351 Fragment Hits. *Structure* 1–12 (2016). doi:10.1016/j.str.2016.06.010
- 352 14. Holton, J. M., Classen, S., Frankel, K. A. & Tainer, J. A. The R-factor gap in macromolecular  
353 crystallography: an untapped potential for insights on accurate structures. *FEBS J.* **281**, 4046–  
354 4060 (2014).
- 355 15. Murshudov, G. N. *et al.* REFMAC 5 for the refinement of macromolecular crystal structures.  
356 *Acta Crystallogr. Sect. D Biol. Crystallogr.* **67**, 355–367 (2011).

357

358

## 359 **Supporting information**

### 360 **S1. Crystallographic Information for Examples**

361 The crystallographic parameters for each of the models used in the examples are listed in Table S1-  
362 Table S4. All models are refined with phenix.refine<sup>11</sup> using the standard settings. All phase differences  
363 are calculated with cphasematch<sup>10</sup> from the model phases as output by phenix.refine, relative to the  
364 ensemble-model phases. Occupancy refinement was performed on all models, except for the ground-  
365 state-only model. When multiple conformations were modelled, the occupancies are constrained to sum  
366 to unity.

### 367 **S2. Validation Radar Plots**

368 Standard validation plots are generated by recording the density scores radially on the graph axes and  
369 connecting these points with lines. For the comparative plots (Figure 4), the axes are re-scaled such that  
370 the limits are the minimum and maximum of the metric scores. For normal validation plots (Figure 6),  
371 the limits of each of the scores are shown in Table S5. These plots can be generated using the  
372 giant.score\_model script distributed as part of the giant package within the panddas package, available  
373 as part of CCP4<sup>10</sup>.

374 **Table S1** Crystallographic parameters and ligand model scores for the model in Section 4.1.

---

<b>Model</b>	<b>Mean Phase Diff. (°)</b>	<b>R-work/ R-free</b>	<b>Occ</b>	<b>RSCC</b>	<b>RSZD</b>	<b>RSZO/ OCC</b>	<b>B-factor Ratio</b>	<b>RMSD (Å)</b>
Solvent Only	2.92	0.129 / 0.171	-	n/a	n/a	n/a	n/a	n/a
Ligand Only	9.97	0.147 / 0.195	0.79	0.44	4.3	0.76	3.54	0.26
Ensemble	-	0.127 / 0.171	0.26	0.87	0.5	5.38	1.47	0.01
Degraded Ensemble	24.17	0.241 / 0.290	0.27	0.77	1.0	4.81	1.40	0.05

---

375

376 **Table S2** Crystallographic parameters and ligand model scores for the model in Section 4.2.

---

<b>Model</b>	<b>Mean Phase Diff. (°)</b>	<b>R-work/ R-free</b>	<b>Occ</b>	<b>RSCC</b>	<b>RSZD</b>	<b>RSZO/ OCC</b>	<b>B-factor Ratio</b>	<b>RMSD (Å)</b>
Solvent Only	2.95	0.183 / 0.217	-	n/a	n/a	n/a	n/a	n/a
Ligand Only	4.15	0.184 / 0.215	0.68	0.92	3.6	1.62	1.41	0.20
Ensemble	-	0.182 / 0.216	0.41	0.96	1.6	3.41	1.04	0.02
Degraded Ensemble	31.06	0.311 / 0.363	0.29	0.90	0.1	1.72	1.18	0.70

---

377

378 **Table S3** Crystallographic parameters and ligand model scores for the model in Section 4.3.

---

<b>Model</b>	<b>Mean Phase Diff. (°)</b>	<b>R-work/ R-free</b>	<b>Occ</b>	<b>RSCC</b>	<b>RSZD</b>	<b>RSZO/ OCC</b>	<b>B-factor Ratio</b>	<b>RMSD (Å)</b>
Solvent Only	3.86	0.157 / 0.219	-	n/a	n/a	n/a	n/a	n/a
Ligand Only	4.38	0.164 / 0.222	0.80	0.78	3.40	2.75	1.23	0.16
Ensemble	-	0.159 / 0.220	0.51	0.83	1.20	4.31	1.13	0.03
Degraded Ensemble	28.48	0.274 / 0.332	0.59	0.71	0.50	2.54	1.19	0.17

---

379

380 **Table S4** Crystallographic parameters and ligand model scores for the model in Section 4.4.

---

<b>Model</b>	<b>Mean Phase Diff. (°)</b>	<b>R-work/ R-free</b>	<b>Occ</b>	<b>RSCC</b>	<b>RSZD</b>	<b>RSZO/ OCC</b>	<b>B-factor Ratio</b>	<b>RMSD (Å)</b>
Solvent Only	4.22	0.186 / 0.216	-	n/a	n/a	n/a	n/a	n/a
Ligand Only	2.20	0.183 / 0.213	0.89	0.95	2.00	4.38	1.26	0.03
Ensemble	-	0.182 / 0.212	0.84	0.96	1.60	5.95	1.20	0.01
Degraded Ensemble	34.46	0.341 / 0.380	0.77	0.91	0.10	3.77	1.14	0.07

---

381

---

382 **Table S5 Radar plot axes limits.** The limits and length scales for the radial axes are defined here.  
383 The inner limit defines the value at which the plotted line will begin to move away from the centre of  
384 the plot. The outer limit defines the values at which the plotted line will reach the end of the radial axis,  
385 and be plotted outside the graph area. If a metric is inverted, large values will be plotted closer to the  
386 centre of the radar plot, and smaller values will be plotted further from the centre.

---

<b>Metric</b>	<b>Inner Limit</b>	<b>Outer Limit</b>	<b>Inverted</b>
RSCC	0.85	0.6	Yes
RSZD	1.5	4	No
RSZO/OCC	2	0	Yes
B-factor Ratio	1	3	No
RMSD	0	1.5	No

---

387

